Axonal excitability changes and acute symptoms of oxaliplatin treatment: *in vivo* evidence for slowed sodium channel inactivation.

Rikke Heide [a, b], Hugh Bostock [c], Lise Ventzel [d], Peter Grafe [e], Joseph Bergmans [f]

Anders Fuglsang-Frederiksen [a], Nanna B. Finnerup [b,1], Hatice Tankisi [a,1]

[a] *Department of Clinical Neurophysiology, Aarhus University Hospital, Aarhus, Denmark*

[b] *Danish Pain Research Center, Department of Clinical Medicine, Aarhus University, Aarhus, Denmark*

[c] *Institute of Neurology, Queen Square House, London, United Kingdom*

[d] *Department of Clinical Oncology, Aarhus University Hospital, Aarhus, Denmark*

[e] *Institute of Physiology, Ludwig-Maximilians University Munich, Munich, Germany*

[f] *Laboratory of Clinical Neurophysiology, Faculty of Medicine, University of Louvain, Brussels, Belgium*

[1] These authors contributed equally to the article.

Corresponding author:

Hatice Tankisi

Department of Neurophysiology

Aarhus University Hospital

Nørrebrogade 44, 8000 Aarhus C, Denmark

Tel.: +45 78 46 24 31

Fax: +45 78 46 31 40

E-mail address: hatitank@rm.dk

Abstract

Objective: Neurotoxicity is the most frequent dose-limiting side effect of the anti-cancer agent oxaliplatin, but the mechanisms are not well understood. This study used nerve excitability testing to investigate the pathophysiology of the acute neurotoxicity.

Methods: Questionnaires, quantitative sensory tests, nerve conduction studies and nerve excitability testing were undertaken in 12 patients with high-risk colorectal cancer treated with adjuvant oxaliplatin and in 16 sex- and age-matched healthy controls. Examinations were performed twice for patients: once within 3 days after oxaliplatin treatment (post-infusion examination) and once shortly before the following treatment (recovery examination).

Results: The most frequent post-infusion symptoms were tingling paresthesias and cold allodynia. The most prominent nerve excitability change was decreased superexcitability of motor axons which correlated with the average intensity of abnormal sensations (Spearman Rho=0.80, $p<0.01$). The motor nerve excitability changes were well modeled by a slowing of sodium channel inactivation, and were proportional to dose/m^2 with a half-life of about 10d.

Conclusions: Oxaliplatin induces reversible slowing of sodium channel inactivation in motor axons, and these changes are closely related to the reversible cold allodynia. However, further studies are required due to small sample size in this study.

Significance: Nerve excitability data provide an index of sodium channel dysfunction: an objective biomarker of acute oxaliplatin neurotoxicity.

Keywords: Nerve Excitability Testing, Chemotherapy, Neuropathy, Quantitative Sensory Tests, Oxaliplatin toxicity, Sodium channel dysfunction.

Highlights:

- Symptoms after oxaliplatin infusion correlate with nerve excitability findings.
- Oxaliplatin induces a slowing of sodium channel inactivation in motor nerve fibres.
- Motor nerve superexcitability may be a good biomarker of acute oxaliplatin neurotoxicity.

1. Introduction

Oxaliplatin is a third-generation platinum analog used for the treatment of solid cancers, in particular as primary and adjuvant treatment of advanced and high-risk colorectal cancer (DCCG, 2015). Neurotoxicity is a frequent and often dose-limiting side effect of oxaliplatin treatment (Gamelin et al., 2002, Argyriou et al., 2013). Oxaliplatin is unique among platinum analogs, as it induces two clinically different types of peripheral neuropathy. One type is a commonly occurring acute neurotoxicity with transient paresthesia, typically triggered by cold exposure, and muscle spasms in the limbs and jaw. The symptoms develop immediately during infusion and usually resolve within days and before the next cycle of oxaliplatin. Symptoms may increase in both severity and duration with repeated administrations (Pachman et al., 2015). Acute transient symptoms occur in nearly all patients (Wilson et al., 2002; Argyriou et al., 2013; Ventzel et al., 2015, 2016). In contrast, the second type, which is a chronic neuropathy, develops with increasing cumulative dose (Beijers et al., 2014, 2015) and is characterized by sensory loss and paresthesia in a stocking and glove-distribution, eventually progressing to sensory ataxia (Land et al., 2007; Mols et al., 2013; Beijers et al., 2014, 2015).

Conventional nerve conduction studies (NCS) cannot be used to assess early nerve dysfunction (Lehky et al., 2004) and do not reveal abnormalities until axonal loss or demyelination or both are well established, i.e. weeks or months after exposure to a neurotoxic drug. Nerve excitability testing provides complementary information to conventional NCS and may be used to infer the activity of a variety of ion channels, energy-dependent pumps, and ion exchange processes activated during the process of impulse conduction (Krishnan et al., 2009; Barnes, 2012; Kiernan et al., 2013).

The pathophysiological mechanisms of acute oxaliplatin-induced peripheral neuropathy are not yet fully understood. Studies examining axonal excitability tests (Bostock et al., 1998; Kiernan et al., 2000) have suggested abnormal functioning of axonal voltage-gated Na^+ channels in both motor and sensory axons in patients in the acute phase following oxaliplatin treatment (Park et al., 2009a, 2009b, 2011; Park et al., 2012). However, these changes have not been correlated to patients' symptoms. The purpose of the present study was to investigate the underlying mechanisms of acute oxaliplatin-induced neuropathy by examining sensory and motor axonal excitability changes and correlating these to sensory symptoms and signs. Excitability parameters in the acute phase were compared to parameters after partial recovery and to healthy controls, and mathematical modeling of the excitability changes was used to provide an objective index of sodium channel dysfunction.

2. Methods

2.1. Study population

Patients were consecutively recruited from the Department of Oncology, Aarhus University Hospital, Denmark, from May 2015 to January 2016. All patients of at least 18 years and treated with standard adjuvant oxaliplatin (XELOX) after high-risk colorectal cancer (stage II or stage III) (DCCG, 2015) or enrolled in a protocol receiving two cycles of XELOX as neoadjuvant treatment were eligible. Sex- and age-matched healthy controls were recruited by announcement. Patients with conditions that might cause neuropathy (other than the current oxaliplatin treatment) such as known metastatic cancer, previous treatment with chemotherapy, diabetes, renal failure, medicine that may induce neuropathy, alcohol abuse, chronic pain not related to the oxaliplatin treatment above 5 on a 0-10 numerical rating scale (NRS),

and patients who did not read, speak, or understand Danish were excluded. Healthy controls were excluded if they had clinical signs of carpal tunnel syndrome or had used analgesics in the past 7 days. NCS of the median nerve were performed in both patients and healthy controls, and subjects were excluded if they had electrophysiological signs of carpal tunnel syndrome.

All subjects gave written informed consent to the procedures, and the study was approved by the Danish National Committee on Biomedical Research Ethics in Central Denmark Region (no. 1-10-72-414-14) and the Danish Data Protection Agency (no 1-16-02-279-15).

2.2. Study design

Patients were recruited while they were hospitalized to receive one of the first cycles of chemotherapy. The XELOX regimen included oxaliplatin (130 mg/m^2) given intravenously over 2 hours every 3 weeks followed by oral capecitabine (1000 mg/m^2) twice a day for 14 days. Patients receiving two cycles of neoadjuvant oxaliplatin were examined through one of the first two cycles of chemotherapy before surgery.

The first examination was performed within the first 3 days after one of the first three cycles of oxaliplatin (post-infusion examination). The second examination was performed in the last week before the next cycle (recovery examination), which corresponded to a 2-week interval. Patients receiving neoadjuvant oxaliplatin were examined again before the next cycle. One patient discontinued chemotherapy and was scheduled for surgery; in this case the second examination was done after surgery and 53 days after the first examination. No patients received chemotherapy between the first and second examination. One patient died before the second examination, and recovery data were therefore obtained from 11 patients.

Healthy controls were examined on one occasion.

2.3. Clinical examination and questionnaires

At the first examination, patients' medical history was obtained and clinical and neurological examinations were performed. Patients were asked if they had experienced new onset pain or non-painful abnormal sensations (paresthesia or dysesthesia) during the past 24 hours, and the average intensity during the past 24 hours was assessed using an NRS (Numerical Rating Scale) ranging from 0 to 10, with 0 being no pain/abnormal sensations and 10 being the worst pain/sensation imaginable. The patients completed the Neuropathic Pain Symptom Inventory (NPSI © 2004. Bouhassira D, all rights reserved), which is a self-administered questionnaire specifically designed to evaluate different symptoms of neuropathic pain (Bouhassira et al., 2004), and a specific questionnaire for assessing chemotherapy-induced sensory symptoms addressing the upper extremity, the lower extremity, and the orofacial area (Leonard et al., 2005).

2.4. Sensory examination

The temperature in the examination room was kept between 21°C and 25°C, and the basal skin temperature was measured with an infrared thermometer at the site of examination.

Cold-evoked symptoms were assessed using a cold metal cylinder (Ventzel cylinder, Denmark). Participants lifted and held a solid metal cylinder, which had been kept in the refrigerator for at least 12 hours, in the hand for 10 seconds (temperature ~ 6°C) (Ventzel et al., 2015). Hereafter, the participants rated the cylinder as either freezing cold, cold, neutral, warm or burning warm. The participants also rated pain, unpleasantness, and pricking on the NRS (0-10).

Quantitative sensory testing (QST) was done with the patient lying relaxed in a bed in a quiet room during daytime. Tests were performed at the thenar eminence of the dominant hand. Using the QST protocol of the German Research Network on Neuropathic Pain (DFNS) (Rolke et al., 2006a), the following parameters were tested: vibration detection threshold (VDT), cold detection threshold (CDT), cold pain threshold (CPT), warm detection threshold (WDT), heat pain threshold (HPT), thermal sensory limen (TSL), and mechanical pain threshold (MPT). Thermal stimuli were applied using the Thermal Sensory Analyzer (TSA, Medoc, Israel) with a contact area of 3 x 3 cm and cut-off temperatures of 0°C and 50°C (Rolke et al., 2006b). All parameters were determined by repeated measurements as outlined within the standardized and validated QST protocol (Rolke et al., 2006a).

2.5. Neurophysiological examinations

Neurophysiological examinations were undertaken with the subject comfortably seated or lying in a bed with the arm placed on a pillow for examination. The subject's hand and forearm were cleansed with Nuprep skin prep gel and alcohol.

2.5.1. Nerve conduction studies

Conventional sensory and motor NCS of the median nerve were undertaken using the surface electrode technique. Keypoint EMG equipment version 2.11 (Dantec, Skovlunde, Denmark) was used. The evaluated sensory NCS parameters were the conduction velocity, duration and base to peak amplitude in the second or third digit with antidromic stimulation. The motor NCS parameters recorded in the abductor pollicis brevis muscle were distal motor latency, conduction velocity at forearm, peak to peak amplitude, duration and minimum F-wave latency. The duration of the

compound sensory nerve and muscle action potentials was determined at 50% of the base to peak amplitude.

2.5.2. Nerve excitability tests

Motor and sensory nerve excitability tests were done in the median nerve. Stimulation at the wrist and recording from abductor pollicis brevis muscle were controlled by the Qtrac software (Institute of Neurology, University College London, London, distributed by Digitimer Ltd at www.digitimer.com) and stimulus current was applied using an isolated linear bipolar constant current stimulator (DS5, Digitimer Ltd). Stimulations were made with non-polarizable electrodes and an anode electrode placed 10 cm proximal to the stimulation electrode, not over the nerve. A ground electrode was placed at the dorsum of the hand. Compound motor action potentials (CMAP) were recorded in the abductor pollicis brevis muscle with the active electrode over the motor point and a reference electrode placed 4 cm distally. Compound sensory action potentials (CSAP) were recorded from the second digit (in one patient the third digit due to amputation of the second digit) using Velcro ring electrodes placed at the proximal and distal interphalangeal joints for recording and reference, respectively. The skin temperature was measured and kept above 32°C. Multiple excitability measurements were made with the TRONDNF protocol, in which 'thresholds' were tracked as the stimuli required to elicit a target response amplitude that was 40% of maximal. The measurements comprised: 1) strength duration time constant (SDTC), 2) threshold electrotonus (TE) with 100 ms polarizing currents set to +/-40% and +/- 20% of control threshold current, 3) recovery cycle of percentage changes in threshold following a supramaximal stimulus (RC) and 4) current–threshold relationship (I/V), consisting of the threshold changes after 200 ms of polarizing current, varied between 50% and -100% of control threshold current.

Additionally, in a subset of the healthy control subjects, recovery cycles were recorded with two supramaximal conditioning stimuli, 4 ms apart, using the RC2C option in the TRONDNF protocol. Superexcitability was measured by the QtracP software as the minimum mean of 3 adjacent points in the recovery cycle for inter-stimulus intervals less than 12 ms, and subexcitability as the maximum mean of 3 adjacent points at longer intervals and relative refractory period (RRP) as the interpolated inter-stimulus interval at which the nerve first became superexcitable. In the case that the nerve never became superexcitable, superexcitability was scored as zero and RRP was undefined.

2.5.3. Modeling of nerve excitability data

To aid interpretation of the nerve excitability data, the full set of excitability measurements was compared with a previously established mathematical model, which interprets the waveforms recorded as due to the interaction of membrane potential and nodal and internodal ion channels (Kiernan et al., 2005; Howells et al., 2012; Boerio et al., 2014). The MEMFITS option in the Qtrac software was used to find the changes in the normal motor axon model that best fitted the mean post-infusion recordings from motor axons, using a least squares method (Kiernan et al., 2005). For each measurement in the Trond protocol, the discrepancy between the model and the recordings was calculated as: [(xm -xn)/sn] 2, where xm is the threshold of the model, xn the mean and sn the standard deviation of the thresholds for the real nerves. The weights for the measurements within each test were the same but the weights for each test were different (strength-duration relationship = 0.5, threshold electrotonus = 2, current/threshold relationship = 1, recovery cycle = 1). Accordingly, the recently published model of motor nerve excitability (Howells et al., 2012) was first adjusted by small changes to all parameters to optimize the fit to the

healthy control recordings. Then, each parameter in the model was tested in turn to see how well it reduced the discrepancy between the recordings and the model, calculated as described above. The parameters tested included those describing the slow potassium channels, and also the gating of sodium channels and the percentage of non-inactivating (persistent) sodium channels, since these have been implicated in previous studies (Adelsberger et al. 2000, Sittl et al. 2012). With each parameter change, the resting membrane potential was recalculated, since many of the changes (especially potassium conductance and persistent sodium conductance) affected the resting potential.

2.6. Statistical analysis

Post-infusion and recovery nerve excitability parameters were compared within individuals, and data from both examinations were compared with data from controls. The results of the nerve excitability parameters were correlated to the most common symptoms: evoked pain to holding the 6°C solid metal cylinder for 10 seconds and abnormal sensations (average intensity over the past 24 hours, measured on the NRS). Data were analyzed using paired t-tests when comparing post-infusion and recovery data, and unpaired t-tests when comparing post-infusion or recovery data with data from healthy controls. If data did not follow normal distribution, data were analyzed using either Wilcoxon signed rank test for paired data or Mann-Whitney *U* test for unpaired data. Correlations were made by Spearman's correlation coefficient, except that linear correlation was used to assess the percentages of variance accounted for by time-adjusted oxaliplatin dose. Fischer's Exact test and McNemar's test were used for dichotomous data. Stata/IC 12.1 (StataCorp LP, College Station, TX, USA) was used for statistical analysis not involving nerve excitability data and Qtrac was used for statistical analysis of nerve excitability data. All estimates were expressed as mean ±

SD or median and inter quartile range for non-parametric data. p-values < 0.05 were considered significant.

3. Results

3.1. Clinical characteristics

A total of 12 patients and 16 healthy controls were recruited for the study. There was no difference in the distribution of gender (female patients: 6/12, female controls: 9/16, p = 0.74), age (patients: 57.2 (11.9) years, controls: 57.8 (11.8) years, p = 0.89), height (patients: 172.3 (12.7) cm, controls: 172.8 (9.6) cm, p = 0.91) and weight (patients: 78.0 (24.2) kg, controls: 68.5 (14.1) kg, p = 0.20) between patients and healthy controls. Clinical characteristics of patients are listed in Table 1.

All patients reported development of acute neurotoxic symptoms. Eleven patients reported abnormal non-painful sensations within the past 24 hours at the post-infusion examination with an average intensity of 5.3 (2.5), while this was reported by two patients at the recovery examination (Table 2). The most frequent symptoms using the oxaliplatin questionnaires after oxaliplatin treatment were tingling paresthesia in the hands (100%), feet (42%), and orofacial area (50%), throat discomfort (100%), jaw pain (42%), and heavy legs (50%). On the NPSI, pins and needles/tingling were the most severe symptom (NRS 3.7 (2.2)) (Table 2). Symptoms were partly reversed at the recovery examination, where fewer patients experienced neurotoxic sensory symptoms and in all cases to a smaller degree than at the post-infusion examination (Table 2).

3.2. Quantitative Sensory Testing (QST)

There was no difference in the room or skin temperature at the first and the second examination (Room temperature: First 22.3 ± 0.9°C, second 22.7 ± 0.9°C, p = 0.20. Skin temperature: First 34.1 ± 1.0°C, second 33.7 ± 0.9°C, p = 0.15). Patients experienced significantly more pain, unpleasantness, and pricking with cold at the post-infusion than at the recovery examination and compared with healthy controls (Fig. 1). In addition, patients experienced significantly more pain and unpleasantness at the recovery examination than controls (Fig. 1). All patients at the post-infusion examination, 82% at recovery examination, and 13% of healthy controls rated the cylinder as "freezing cold" rather than cold ($p < 0.001$ post-infusion vs controls, $p = 0.001$ recovery vs controls, and $p = 0.02$ post-infusion vs recovery). Two patients could not hold the cylinder for the full 10 seconds at the post-infusion examination (released grip after 3 and 5 seconds respectively).

CPT was significantly lower (more cold pain sensitive) at the post-infusion compared with the recovery examination (16.6 ± 7.9°C, 11.6 ± 7.7°C, p = 0.02) (Fig. 2). There were no differences in other QST parameters (Fig. 2).

3.3. Conventional electrophysiological examinations

No differences were seen in CMAP or CSAP amplitudes between patients at the post-infusion and the recovery examination (CMAP: Post-infusion: 13.8 ± 3.5 mV, recovery: 14.7 ± 3.7 mV, p = 0.2, CSAP: Post-infusion: 18.1 μV, recovery: 18.6 μV p = 0.7) or in comparison with healthy controls (CMAP: 15.1 ± 5.0 mV, p = 0.4, CSAP: 18.6 μV, p = 0.8). Neither were any differences seen when comparing duration of CMAP or CSAP between post-infusion and recovery examinations (CMAP: Post-infusion: 5.2 ± 0.8 ms, recovery: 5.1 ± 0.8 ms, p = 0.8, CSAP: Post-infusion: 0.7 ± 0.1 ms, recovery: 0.7 ± 0.1 ms, p = 0.8) or in comparison with healthy controls (CMAP:

5.2 ± 0.8 ms, p = 0.7, CSAP: 0.8 ± 0.2 ms, p = 0.5). The results indicate no axonal loss in the acute phase after oxaliplatin administration.

There were no signs of repetitive discharges in CSAPs. In contrast, nine patients showed repetitive motor discharges in post-infusion recordings.

3.4 Nerve excitability tests

3.4.1. Motor nerve excitability

Motor nerve excitability measurements were compared between controls, post-infusion and recovery groups in Table 3, and excitability waveforms are illustrated in Fig. 3A-D. The most conspicuous difference between the post-infusion and recovery measurements for the 11 patients for whom paired comparisons could be made were in the higher thresholds during the recovery cycle (Fig. 3D), with a highly significant reduction in superexcitability (p=0.00013) and increase in late subexcitability (p=0.0032) in the post-infusion examinations. The post-infusion recordings also had higher electrical threshold and rheobase and lower strength-duration time constant. In all of these changes, the recovery recordings were closer to the healthy controls than the post-infusion recordings. The differences in superexcitability and subexcitability between post-infusion recordings and healthy controls are shown by the scatter plot in Fig. 3E. There is a small overlap, but the post-infusion recordings differed so substantially from the healthy controls that they could be separated completely by several pairs of excitability measurements, e.g. superexcitability(%) vs peak depolarizing electrotonus (Fig 3F), while the recovery measurements bridged the two groups.

3.4.2. Sensory nerve excitability

Table 4 and Figure 4A-D show the sensory nerve excitability measurements corresponding to the motor excitability measurements in Table 3 and Fig. 3A-D. Although there was a significant increase in superexcitability between the post-infusion and recovery recordings, the similarity in mean post-infusion values of superexcitability and subexcitability to the healthy controls was in marked contrast to the motor nerves. The scatter plots in Figs. 4E and 4F, plotted with similar scaling as Figs. 3E and 3F, show that the failure to detect a post-infusion abnormality in the sensory nerves was not due to any increased variability in the sensory recordings. However, like the motor axons, threshold and rheobase were higher for the post-infusion examination, while strength-duration time constant was shorter.

3.4.3. Motor nerve recovery cycle and repetitive discharges

One possible explanation for the changes in recovery cycle induced by oxaliplatin in motor fibres is that normal impulse transmission is disrupted by repetitive discharges originating in the nerve terminals, which can resemble neuromyotonia (Wilson et al., 2002). To test this possibility, we compared the early changes in the recovery cycle with the repetitive discharges evoked by the supramaximal conditioning stimuli. Examples are illustrated in Figure 5. In the top row, showing superimposed waveforms to 50 supramaximal stimuli, the small circles indicate the first clear repetitive discharges, whereas the large circles indicate F responses. The distances between the vertical lines, indicating the latencies of the first repetitive discharges, averaged 4.8 ± 1.5 ms (mean ± SD, range 3.2 - 7.3 ms) for the 9 post-infusion patients showing multiple action potentials. In each case, the thresholds in the recovery cycle were abnormally high before this interval, and therefore before any collision with an antidromically conducted impulse was possible. Also, it can be seen that the proportion of motor axons discharging repetitively was small, comparable with those

generating F responses, so that any effect of the collisions on thresholds would also be small (see Discussion).

Figure 5 (bottom row) also compares the recovery cycles following oxaliplatin treatment with the recovery cycles following two conditioning stimuli, 4 ms apart (open triangles). They show a clear similarity in waveform, with the example in Fig. 5B superimposed almost perfectly on the mean recovery cycle after two supramaximal conditioning stimuli. This remarkable correspondence suggests that very similar membrane changes are involved. The difference between recovery cycles with one and multiple conditioning stimuli is known to depend primarily on the activation of slow potassium currents (Bergmans, 1970; Schwarz et al., 2006). The results in Fig. 5 therefore indicate that neither the timing nor extent of repetitive discharges could account for the changes in motor recovery cycles, but that these could be explained by additional activation of slow potassium currents at the site of stimulation. To understand how this could have occurred, we used mathematical modeling to explore how oxaliplatin could change the axonal membrane properties to bring this about.

3.4.4. Modeling of motor nerve excitability changes

The extent of the discrepancy reductions are illustrated in Figure 6E for those parameters that reduced the discrepancy by 1% or more. (N.B. The percentage of persistent sodium channels does not occur in this list, since changing this parameter did not reduce the discrepancy at all.) It can be seen that much the best improvement in fit was achieved by a change in Aah, the rate of inactivation of sodium channels. Reducing this rate by 37.3% reduced the discrepancy by 62.5%, whereas no other single parameter changed reduced the discrepancy by more than 12%. The changes in the model excitability waveforms produced by slowing sodium channel inactivation

by 37% are illustrated in Figure 6A-E, and show a highly selective action on the recovery cycle.

The effects of slowing sodium channel inactivation on the recovery cycle are shown in more detail in Figure 7. Fig. 7A shows the recovery cycles of the 12 post-infusion recordings superimposed, and Fig. 7B shows modeled recovery cycles for inactivation rates from 90% to 30% of normal. Slowing sodium channel inactivation slows the recovery phase of the action potential, thus broadening it (Fig. 7C), and increasing the activation of slow (K_v7) potassium channels, which causes an increased hyperpolarizing afterpotential (Fig. 7D), reduced superexcitability and increased late subexcitability.

If oxaliplatin selectively slows sodium channel inactivation in motor fibres, one might expect it to also slow sodium channel inactivation in sensory fibres, since the major sodium channel isoform in each case is $Na_v1.6$ (Caldwell et al., 2000). However, applying similar changes in the parameter Aah in the model for sensory fibres (Howells et al., 2012) produced changes in the sensory nerve recovery cycle similar to those in Fig. 6, in contrast to the recorded recovery cycles (Fig. 4).

3.5. Correlations

3.5.1. Motor nerve superexcitability, subexcitability and acute sensory symptoms

The sensory abnormalities that best distinguished the post-infusion from recovery examinations, with the greatest difference in median NRS (scale 1-10) and by Wilcoxon signed rank test, were the responses to the cold cylinder as in Fig. 1 and the average of unpleasant sensations over 24 hours. These NRS values at the first examination each correlated significantly with motor axon superexcitability: average unpleasantness (Rho=0.797, p=0.0020), cold cylinder pricking (Rho=0.640, p=0.024),

cold cylinder pain (Rho=0.628, p=0.028), cold cylinder unpleasantness (Rho=0.640, p=0.024). The corresponding figures for motor axon late subexcitability were: average unpleasantness (Rho=0.762, p=0.0040), cold cylinder pricking (Rho=0.685, p=0.014), cold cylinder pain (Rho=0.670, p=0.017), cold cylinder unpleasantness (Rho=0.685, p=0.014).

3.5.2. Superexcitability, sensory symptoms and time-adjusted oxaliplatin dose

The range of different acute drug effect on superexcitability shown in Fig. 7A seemed surprising, considering that the measurements followed single doses that only varied between 94 and 136 mg/m^2. Previous studies have shown that the cold allodynia induced by oxaliplatin declines over a period of days. To help to explain the differences in superexcitability, we assumed a simple model in which the change was initially proportional to the dose and decayed exponentially, described by a half-life of *h* days. On this model, the time adjusted dose *D* should be related to the original dose D by the relationship $D = D \times 2^{(-t/h)}$ where t is the time in days after infusion. For the second and subsequent infusion, this expression should be summed over all infusions, i.e. time-adjusted total dose = $\sum D \times 2^{(-t/h)}$. Using this relationship, we calculated the linear correlations between superexcitability and time-adjusted total dose per surface area for half-times between 1 and 50 days, using the data from all the 23 patient examinations (Figure 8A). There was a broad maximum in the correlations, peaking at a half-life of 7-10 days. Fig. 8C shows the scatter plot of values for superexcitability and estimated dose/m^2 for a half-life of 10 days. The correlation coefficient was 0.813, indicating that this relationship accounts for 66% of the variance in superexcitability, and the regression line cuts the *y* axis at a superexcitability of -24.5%, close to the value expected for a zero dose, since superexcitability in the healthy controls averaged -23.2%.

Fig. 8B shows similar calculations for the two most abnormal sensations induced by oxaliplatin: cold cylinder pricking and average unpleasant sensations over 24 hours. In each case, the correlation with time-adjusted oxaliplatin dose was highest for a half-life of about 10 days. The correlation reached a value of 0.957 for cold cylinder pricking, indicating that 92% of the variance in this measurement was accounted for by this simple model. Comparison between Fig. 8A and Fig. 8B shows that there is a good correspondence in the time course of the effect of oxaliplatin on sodium channel inactivation and the time course of its effect on acute neurotoxic symptoms.

3.5.3. Sensory nerve excitability and acute sensory symptoms

In contrast to the correlations with motor nerve excitability changes, we found no significant correlations between pain from holding the cylinder or intensity of abnormal sensations and sensory axonal excitability. The correlation coefficients and p-values for post-infusion superexcitability correlated to holding the cylinder are: average unpleasantness (Rho= -0.032, p=0.922), cold cylinder pricking (Rho=0.026, p=0.936), cold cylinder pain (Rho=0.038, p=0.908) and cold cylinder unpleasantness (Rho=0.026, p=0.936).

4. Discussion

There have already been a number of papers describing nerve excitability studies in patients receiving oxaliplatin treatment (Krishnan et al. 2005, 2006; Park et al. 2009a, 2009b, 2011; McHugh et al. 2012). Where this study breaks new ground is a) in providing evidence for the role of slowed sodium channel inactivation in the changes in motor nerve excitability, b) in demonstrating the close relationship between the acute changes in the motor nerve recovery cycle and the acute sensory symptoms, and c) in relating both of these acute changes to the patient treatment history.

This study has confirmed the paradoxical nature of the acute effects of oxaliplatin on nerve excitability: although it is a sensory hyperexcitability that is the most serious acute side-effect of oxaliplatin treatment, it is motor axons that display the most marked excitability abnormalities. The reversible changes in the recovery cycle of motor axons were very similar to those previously described by Krishnan and colleagues (Krishnan et al., 2005, 2006), although we did not find significant changes in RRP. (This comparative lack of sensitivity may have been in part because we made no baseline examinations, so we were unable to compare pre- and post-infusion recordings directly, in part because of the variable timing of the post-infusion recordings (1-3d) and in part because of the limited number of patients). Park and colleagues (Park et al., 2009b) demonstrated more subtle acute effects of oxaliplatin on sensory fibres. We found an increase in sensory superexcitability between the 1st and 2nd examinations, but no significant differences from healthy controls. The sensory changes indicated by Park et al. were cumulative, rather than reversible, and after many drug cycles were clearly related to the chronic sensory neuropathy. Although the recovery cycle changes were quite different between motor and sensory fibres, some excitability changes were similar: thresholds and rheobases were significantly increased at post-infusion and partly normalized at recovery, whereas SDTCs were significantly reduced post-infusion. Since these excitability parameters are those most dependent on current access to the axons, and did not correlate with the other, dose-dependent excitability measurements, interpretation is uncertain.

4.1. Biophysical basis of changes in motor nerve excitability

Krishnan et al. (2005, 2006) found that oxaliplatin induced an increase in refractoriness in motor axons, without changes in threshold electrotonus or SDTC,

and concluded that oxaliplatin neurotoxicity is mediated through an effect on nodal voltage-gated sodium channels. Park et al. (2009b) confirmed the increase in refractoriness in motor axons, but found a contrasting decrease in refractoriness in sensory axons. In seeking an explanation for this discrepancy they noted that oxaliplatin has been shown to induce 'neuromyotonic-type' discharges in motor axons (Wilson et al., 2002). They suggested that these might account for the increased refractoriness at short inter-stimulus intervals, since Kuwabara et al. (2001) reported that the refractory period of transmission in normal human motor fibres is prolonged by a period of maximal voluntary contraction. However, the repetitive discharges in neuromyotonia are not associated with any increase in refractoriness (Kiernan et al., 2001). Also, the voluntary activity employed by Kuwabara and colleagues generated an increase in superexcitability, contrasting with the decrease with oxaliplatin. An alternative possibility would be that oxaliplatin-induced repetitive discharges from the motor nerve terminals might raise thresholds during the recovery cycle by colliding with the test volley. We have investigated this possibility (Fig. 5) and found that the repetitive discharges only occur after an interval of *ca* 5 ms, too late to account for the early increase in refractoriness.

In oxaliplatin-treated patients, the proportion of motor axons giving a repetitive discharge to the supramaximal conditioning stimuli was small (Fig. 5, top row), so the antidromic impulses could only have produced a small reduction in superexcitability and increase in late subexcitability. (N.B. Because of the high slope of the stimulus-response curve for motor fibres, a 5% reduction in the number of fibres conducting a second impulse, due to collision with a repetitive discharge, would only be expected to increase threshold by about 1%). The characteristic elevation of the whole of the recovery cycle (increased refractoriness, reduced superexcitability and increased late

subexcitability), which was seen even when there were no repetitive discharges, (as was the case in nearly all of the 2nd examination recordings) requires a different explanation.

Studies of the effects of oxaliplatin on rodent neuronal preparations have provided evidence for a variety of changes in action potentials or sodium channel gating: Adelsberger et al. (2000) reported that the most pronounced effect of oxaliplatin on dorsal root ganglion (DRG) cells was a slowdown of the inactivation kinetics of sodium channels; Sittl et al. (2012), recording from cultured mouse DRG neurons, found enhanced resurgent and persistent sodium currents on cooling in the presence of oxaliplatin. When we modeled the effects of changes in membrane properties on motor nerve excitability, we found that slowing of sodium channel inactivation kinetics alone provided a satisfactory explanation of our patient recordings, since the broadened action potentials had a similar effect on the recovery cycle to a second conditioning impulse, without appreciable effect on electrotonus (Figs. 6,7). The puzzling question of why similar changes were not seen in the large sensory fibres is considered further below (section 4.4).

4.2. Correlation between acute motor nerve changes and acute sensory symptoms

The most severe symptoms of oxaliplatin neurotoxicity are sensory, so it is important to establish how closely the easily measureable acute changes in motor axons are related to the acute sensory symptoms. A novel feature of this study is that it is the first to combine QST, pain questionnaires and cold cylinder tests of cold allodynia with nerve excitability studies. The measurements made in this study were at different times (1-3 and 15-20 days, one patient 53 days) after different oxaliplatin doses (94-136 mg/m^2), and sensory symptoms were compared with motor nerve

superexcitability over these differing treatments. The results show significant correlations, especially with the average unpleasantness, for which half the variation at the first examination was accounted for by the correlation with superexcitability (Rho = 0.797). This correlation was maintained over the 23 observations in both examinations (Rho=0.783). The correlation between superexcitability and pricking pain with the cold cylinder was also significant (1st examination Rho=0.640, both examinations Rho=0.786). This, and the fact that the two phenomena decay over a similar time course (see below), suggest that sodium channel dysfunction may also be responsible for the cold allodynia.

4.3. Relation between acute neurotoxicity and dose history

Another novelty of this study is that the effect of an oxaliplatin dose on motor superexcitability can be modeled quite well on the simple assumption that excitability changes are proportional to the dose/m^2 but decay with a half-life of about 10 days (Fig. 8). Moreover, the same model accounts remarkably well for the variation in NRS scores for cold allodynia. The origin of the long half-life of the oxaliplatin-modified sodium channels is not clear: it might be related to slow dissociation of the oxaliplatin-channel complex, or possibly to the normal turnover rate for peripheral nerve Na channels. Interestingly, although most ultrafiltrable platin is removed from the blood within a day or two (Kern et al., 1999), a 'terminal elimination phase' can be detected with a half-life of 237 hours (Morrison et al., 2000), close to the apparent half-life of the acute neurotoxicity.

Although the correlation coefficients in Fig. 8C,D are high, the confidence limits for the regression lines indicate that a considerable degree of inter-patient variability is not accounted for by the time-adjusted dose. Ehrsson et al. (2002) found a coefficient of variation of only 14% for serum oxaliplatin levels for the same dose/m^2. Other

sources of variation may include differences in access to the axons across the blood-nerve barrier and genetic polymorphisms, as well as the variation intrinsic in individual measurements.

4.4. Differences in oxaliplatin sensitivity of motor and large sensory axons

A puzzling feature of oxaliplatin neurotoxicity, as already mentioned, is that sodium channels in motor axons in the nerve trunk, underneath the stimulating electrode, have their rate of inactivation slowed, whereas nearby sodium channels in Aβ large sensory axons in a similar environment are less affected. There is clear evidence, however, that the major sodium channel isoform at nodes of Ranvier in both motor and sensory axons is $Na_v1.6$ (Caldwell et al., 2000). Differential access to the two axon types seems unlikely, and this raises the possibility that accessory subunits or other channel-binding proteins may differ between nodes in sensory and motor axons and affect the affinity of the $Na_v1.6$ channels for oxaliplatin. Direct evidence comparing the sensitivity of motor and sensory mammalian axons to oxaliplatin is not available in the literature. The oxaliplatin concentrations within the nerve fascicles are unknown, but must be less than the serum concentrations, which according to Ehrsson et al. (2002) reach a maximum of 1.44 μg/ml (=3.6 μM) for a dose of 85 mg/m^2, corresponding to 4.0-5.8 μM for the dose range (94-136 mg/m^2) in this study. The only animal studies reporting action potential broadening at such a low concentration were those of Kagiava et al. (2008, 2013). They recorded intracellularly from rat sciatic axons and found broadened action potentials with oxaliplatin concentrations as low as 5 μM, but their preparation did not allow distinction between motor and sensory axons. Studies on sensory mammalian nerves have used higher concentrations: Adelsberger et al. (2000) recorded broadened rat sural nerve action potentials with 250 μM oxaliplatin; Sittl et al. (2010) used lower concentrations of

oxaliplatin (10-30 μM) in an organ bath, and tested isolated fascicles of human as well as rat sural nerves, but only reported broadened action potentials and after-activity with 30 μM oxaliplatin. Sittl et al. (2012) also found an increase in depolarizing threshold electrotonus in desheathed mouse sural nerve exposed to 100 μM oxaliplatin, suggestive of increased persistent sodium currents and correlated with repetitive activity.

So further animal experiments are required to resolve the question of whether motor and sensory nodes in the nerve trunk have a different sensitivity to oxaliplatin, as our results seem to apply. As to how such a difference in sensitivity could arise, one possibility could be competitive binding by the fibroblast growth factor homologous factor 2B (FHF2B), which is colocalized with $Na_v1.6$ at mature nodes of Ranvier in dorsal root sensory, but not ventral root motor axons (Wittmack et al., 2004), but other possible mechanisms also needs to be explored.

Although the sensory nerve excitability measurements showed no evidence of altered sodium channel gating with oxaliplatin, sensory symptoms are more prominent and reported by a greater fraction of patients than motor symptoms. Although we cannot exclude methodological causes such as technical difficulties in assessing sensory fibers or the relatively low number of subjects, which is a limitation of this study, this may in part be accounted for by the occurrence of Aδ-mediated painful sensations, but patients also report tingling and buzzing sensations, indicating involvement of Aβ fibers. Spontaneous activity in Aβ fibres would not be detectable in our nerve excitability recordings, just as they are not visible in conventional NCS (Campero et al., 1998).

The difference between motor and sensory axons is as marked in their sensitivity to chronic neurotoxicity as it is to the acute neurotoxicity. In chronic neurotoxicity it is

tingling and numbness, caused by Aβ fibres loss, that are the worst symptoms (Pachman et al., 2015). In this and other respects, the chronic oxaliplatin neurotoxicity resembles that induced by cisplatin and other platins, which do not have a specific action on sodium channels, but which accumulate in DRG neurones and may damage the cells by binding to DNA (Ta et al., 2006; Park et al., 2013), or by interfering with microtubule-based axonal transport (Higa et al., 2016).

4.5. Motor nerve superexcitability as a biomarker for oxaliplatin neurotoxicity?

Several studies have shown that sensitivity to acute oxaliplatin neurotoxicity correlates well with sensitivity to chronic neurotoxicity (Pachman et al., 2014; Pachman et al., 2015). In the most long-lasting study, Pachman and colleagues (Pachman et al., 2015) found a good correlation between acute symptoms during the first treatment cycle and the chronic sensory neurotoxicity up to 18 months after cessation of chemotherapy. Nerve excitability measurements are extremely sensitive to the changes in sodium channels responsible for the acute neurotoxicity, and it has reasonably been proposed that they may therefore provide an objective biomarker for the risk of developing chronic nerve damage (Krishnan et al., 2006). While our data strongly support their proposal, it does not follow that prophylactic strategies to reduce the acute neurotoxicity by mitigating the effects on sodium currents can be expected to avert the chronic neurotoxicity. This is because the mechanisms may be quite different, as discussed in the previous paragraph. However, one should remember the small sample size in our study, which limits making clear conclusions. Further studies with larger patient groups are warranted.

1. Acknowledgements

Conflict of interest: HB receives royalties from UCL for sales of his Qtrac software used in this study. The other authors have no potential conflicts of interest.

The study was financially supported mainly by the Lundbeck Foundation. Additionally, Aase and Ejnar Danielsens Foundation, Foundation of Neurological research, Denmark. Hatice Tankisi and Nanna B Finnerup are part of DOLORisk, a European Union's Horizon 2020 research and innovation programme under grant agreement No 633491 supported the project.

Reference List

Adelsberger H, Quasthoff S, Grosskreutz J, Lepier A, Eckel F, Lersch C. The chemotherapeutic oxaliplatin alters voltage-gated Na(+) channel kinetics on rat sensory neurons. Eur J Pharmacol. 2000;406:25-32.

Argyriou AA, Cavaletti G, Briani C, Velasco R, Bruna J, Campagnolo M, et al. Clinical pattern and associations of oxaliplatin acute neurotoxicity: a prospective study in 170 patients with colorectal cancer. Cancer. 2013;119:438-44.

Barnes M. Handbook of Clinical Neurology: Elsevier; 2012.

Beijers AJ, Mols F, Tjan-Heijnen VC, Faber CG, LV vdP-F, Vreugdenhil G. Peripheral neuropathy in colorectal cancer survivors: The influence of oxaliplatin administration. Results from the population-based PROFILES registry. Acta Oncol. 2015;54:463-9.

Beijers AJ, Mols F, Vreugdenhil G. A systematic review on chronic oxaliplatin-induced peripheral neuropathy and the relation with oxaliplatin administration. Support Care Cancer. 2014;22:1999-2007.

Bergmans J. The physiology of single human nerve fibres. Vander; University of Louvain; 1970.

Boerio D, Bostock H, Spescha R, Z'Graggen WJ. Potassium and the excitability properties of normal human motor axons in vivo. PLoS One. 2014;9:e98262.

Bostock H, Cikurel K, Burke D. Threshold tracking techniques in the study of human peripheral nerve. Muscle Nerve. 1998;21:137-58.

Bouhassira D, Attal N, Fermanian J, Alchaar H, Gautron M, Masquelier E, et al. Development and validation of the Neuropathic Pain Symptom Inventory. Pain. 2004;108:248-57.

Caldwell JH, Schaller KL, Lasher RS, Peles E, Levinson SR. Sodium channel Na(v)1.6 is localized at nodes of ranvier, dendrites, and synapses. Proc Natl Acad Sci U S A. 2000;97:5616-20.

Campero M, Serra J, Marchettini P, Ochoa JL. Ectopic impulse generation and autoexcitation in single myelinated afferent fibers in patients with peripheral neuropathy and positive sensory symptoms. Muscle Nerve. 1998;21:1661-7.

DCCG. Danish Colorectal Cancer Group. Retningslinjer for diagnostik og behandling af kolorektalkræft Danish Colorectal Cancer Group2015.

Ehrsson H, Wallin I, Yachnin J. Pharmacokinetics of oxaliplatin in humans. Medical Oncol. 2002;19:261-265.

Gamelin E, Gamelin L, Bossi L, Quasthoff S. Clinical aspects and molecular basis of oxaliplatin neurotoxicity: current management and development of preventive measures. Semin Oncol. 2002;29:21-33.

Howells J, Trevillion L, Bostock H, Burke D. The voltage dependence of I(h) in human myelinated axons. J Physiol. 2012;590:1625-40.

Kagiava A, Kosmidis EK, Theophilidis G. Oxaliplatin-induced hyperexcitation of rat sciatic nerve fibres: an intra-axonal study. Anticancer Agents Med Chem. 2013;13:373-379.

Kagiava A, Tsingotjidou A, Emmanouilides C, Theophilidis G. The effects of oxaliplatin, an anticancer drug, on potassium channels of the peripheral myelinated nerve fibres of the adult rat. Neurotoxicol. 2008;29:1100-1106.

Kern W, Braess J, Bottger B, Kaufmann CC, Hiddemann W, Schleyer E. Oxaliplatin pharmacokinetics during a four-hour infusion. Clin Cancer Res. 1999;5:761-5.

Kiernan MC, Bostock H. Effects of membrane polarization and ischaemia on the excitability properties of human motor axons. Brain. 2000;123 Pt 12:2542-51.

Kiernan MC, Isbister GK, Lin CS, Burke D, Bostock H. Acute tetrodotoxin-induced neurotoxicity after ingestion of puffer fish. Ann Neurol. 2005;57:339-48.

Kiernan MC, Kaji R. Physiology and pathophysiology of myelinated nerve fibers. Handb Clin Neurol. 2013;115:43-53.

Krishnan AV, Goldstein D, Friedlander M, Kiernan MC. Oxaliplatin-induced neurotoxicity and the development of neuropathy. Muscle Nerve. 2005;32:51-60.

Krishnan AV, Goldstein D, Friedlander M, Kiernan MC. Oxaliplatin and axonal Na+ channel function in vivo. Clin Cancer Res. 2006;12:4481-4.

Krishnan AV, Lin CS, Park SB, Kiernan MC. Axonal ion channels from bench to bedside: a translational neuroscience perspective. Prog Neurobiol. 2009;89:288-313.

Kuwabara S, Lin CS-Y, Mogyoros I, Cappelen-Smith C, Burke D. Voluntary contraction impairs the refractory period of transmission in healthy human axons. J Physiol. 2001;531:265-275.

Land SR, Kopec JA, Cecchini RS, Ganz PA, Wieand HS, Colangelo LH, et al. Neurotoxicity from oxaliplatin combined with weekly bolus fluorouracil and leucovorin as surgical adjuvant chemotherapy for stage II and III colon cancer: NSABP C-07. J Clin Oncol. 2007;25:2205-11.

Lehky TJ, Leonard GD, Wilson RH, Grem JL, Floeter MK. Oxaliplatin-induced neurotoxicity: acute hyperexcitability and chronic neuropathy. Muscle Nerve. 2004;29:387-92.

McHugh JC, Tryfonopoulos D, Fennelly D, Crown J, Connolly S. Electroclinical biomarkers of early peripheral neurotoxicity from oxaliplatin. Eur J Cancer Care (Engl). 2012;21:782-9.

Mols F, Beijers T, Lemmens V, van den Hurk CJ, Vreugdenhil G, LV vdP-F. Chemotherapy-induced neuropathy and its association with quality of life among 2- to 11-year colorectal cancer survivors: results from the population-based PROFILES registry. J Clin Oncol. 2013;31:2699-707.

Morrison JG, White P, McDougall S, Firth JW, Woolfrey SG, Graham MA, et al. Validation of a highly sensitive ICP-MS method for the determination of platinum in biofluids: application to clinical pharmacokinetic studies with oxaliplatin. J Pharm Biomed Anal. 2000;24:1-10.

Pachman DR, Qin R, Seisler DK, Smith EM, Beutler AS, Ta LE, et al. Clinical Course of Oxaliplatin-Induced Neuropathy: Results From the Randomized Phase III Trial N08CB (Alliance). J Clin Oncol. 2015;33:3416-22.

Pachman DR, Watson JC, Lustberg MB, Wagner-Johnston ND, Chan A, Broadfield L, et al. Management options for established chemotherapy-induced peripheral neuropathy. Support Care Cancer. 2014;22:2281-95.

Park SB, Goldstein D, Krishnan AV, Lin CS, Friedlander ML, Cassidy J, et al. Chemotherapy-induced peripheral neurotoxicity: a critical analysis. CA Cancer J Clin. 2013;63:419-37.

Park SB, Goldstein D, Lin CS-Y, Krishnan AV, Friedlander ML, Kiernan MC. Acute abnormalities of sensory nerve function associated with oxaliplatin-induced neurotoxicity. J Clin Oncol. 2009a;27:1243-1249.

Park SB, Lin CS, Kiernan MC. Nerve excitability assessment in chemotherapy-induced neurotoxicity. J Vis Exp. 2012;62:10.3791/439.

Park SB, Lin CS, Krishnan AV, Goldstein D, Friedlander ML, Kiernan MC. Oxaliplatin-induced neurotoxicity: changes in axonal excitability precede development of neuropathy. Brain. 2009b;132:2712-23.

Park SB, Lin CS, Krishnan AV, Goldstein D, Friedlander ML, Kiernan MC. Dose effects of oxaliplatin on persistent and transient Na+ conductances and the development of neurotoxicity. PLoS One. 2011;6:e18469.

Rolke R, Baron R, Maier C, Tolle TR, Treede RD, Beyer A, et al. Quantitative sensory testing in the German Research Network on Neuropathic Pain (DFNS): standardized protocol and reference values. Pain. 2006a;123:231-43.

Rolke R, Magerl W, Campbell KA, Schalber C, Caspari S, Birklein F, et al. Quantitative sensory testing: a comprehensive protocol for clinical trials. Eur J Pain. 2006b;10:77-88.

Schwarz JR, Glassmeier G, Cooper E, Kao T, Nodera H, Tabuena D, Kaji R, Bostock H. KCNQ channels mediate the slow K+ current in the rat node of Ranvier. J Physiol. 2006;573,17-34

Sittl R, Carr RW, Fleckenstein J, Grafe P. Enhancement of axonal potassium conductance reduces nerve hyperexcitability in an in vitro model of oxaliplatin-induced acute neuropathy. Neurotoxicology. 2010;31:694-700.

Sittl R, Lampert A, Huth T, Schuy ET, Link AS, Fleckenstein J, et al. Anticancer drug oxaliplatin induces acute cooling-aggravated neuropathy via sodium channel subtype Na(V)1.6-resurgent and persistent current. Proc Natl Acad Sci U S A. 2012;109:6704-9.

Ta LE, Espeset L, Podratz J, Windebank AJ. Neurotoxicity of oxaliplatin and cisplatin for dorsal root ganglion neurons correlates with platinum-DNA binding. Neurotoxicology. 2006;27:992-1002.

Ventzel L, Jensen AB, Jensen AR, Jensen TS, Finnerup NB. Chemotherapy-induced pain and neuropathy: a prospective study in patients treated with adjuvant oxaliplatin or docetaxel. Pain. 2016;157:560-8.

Ventzel L, Madsen CS, Jensen AB, Jensen AR, Jensen TS, Finnerup NB. Assessment of acute oxaliplatin-induced cold allodynia: a pilot study. Acta Neurol Scand. 2015;DOI: 10.1111/ane.12443.

Wilson RH, Lehky T, Thomas RR, Quinn MG, Floeter MK, Grem JL. Acute oxaliplatin-induced peripheral nerve hyperexcitability. J Clin Oncol. 2002;20:1767-74.

Wittmack EK, Rush AM, Craner MJ, Goldfarb MJ, Waxman SG, Dib-Hajj SD. Fibroblast growth factor homologous factor 2B: association with $Na_v1.6$ and selective colocalization at nodes of Ranvier of dorsal root axons. J Neurosci. 2004;24:6765-6775.

Figure legends

Fig. 1. Intensity of pain, unpleasantness and pricking with holding a cold metal cylinder (approximately 6°C) for 10 seconds.

Boxes: interquartile range, whiskers: 10% and 90% percentiles. NRS: Numeric rating scale. * $p < 0.05$ ** $p < 0.01$ *** $p < 0.005$.

Fig. 2. Multiple error bars plot of mean z-score ± SD for QST parameters at post-infusion and recovery examination.

CDT: cold detection threshold; WDT: warm detection threshold; TSL: thermal sensory limen; CPT: cold pain threshold; HPT: heat pain threshold; MPT: mechanical pain threshold; VDT: vibration detection threshold. * $p < 0.05$.

Fig. 3. Motor nerve excitability recordings. Curves: Mean of patients (n = 11), controls (n = 16). Healthy controls (open circles), patients with post-infusion examination (filled triangles), and patients with recovery examination (open squares). A) Current/threshold (I/V) relationship, B) Strength-duration time constant, C) Threshold electrotonus, D) Recovery cycle, E) Subexcitability (%) plotted against superexcitability(%) for post-infusion and healthy controls only, F) Peak depolarizing electrotonus TEd(peak) plotted against superexcitability(%) for all three groups. In E and F the polygons join the limits of the groups.

Fig. 4. Sensory nerve excitability recordings, plotted as for the motor nerves in Fig. 3. Curves: Mean of patients (n = 11), controls (n = 16). Healthy controls (open circles), patients with post-infusion examination (filled triangles) and patients with recovery examination (open squares). A) I/V relationship, B) Strength-duration time constant,

C) Threshold electrotonus, D) Recovery cycle., E) Subexcitability plotted against superexcitability for post-infusion and healthy controls only, F) Peak depolarizing electrotonus TEd(peak) plotted against superexcitability for all three groups.

Fig. 5. Comparison between repetitive discharges and recovery cycles of motor fibres. *Top row*: Superimposed CMAP responses to 50 supramaximal conditioning stimuli illustrated for two post-infusion recordings (A,B) and one recovery recording (C). Small circles indicate first indication of a repetitive discharge (barely visible in C); large circles indicate F-waves. Vertical lines indicate action potential peaks, with separations 7.6 (A), 4.0 (B) and 6.6 ms (C). *Bottom row:* Recovery cycles from same recordings as in top row (filled black circles). Open grey circles and dashed lines indicate mean ± SD for RCs of healthy controls (*n*=16). Open triangles and dashed lines indicate mean ± SD for RCs of healthy controls with 2 conditioning stimuli (*n*=8). Note (a) that abnormal elevation of post-infusion RCs starts before thresholds could be affected by repetitive discharges, and (b) that post-infusion RC in B is indistinguishable from mean RC of healthy controls with 2 conditioning stimuli.

Fig. 6. The changes in the model excitability waveforms produced by slowing sodium channel inactivation by 37% are illustrated in Figure 6A-E, and show a highly selective action on the recovery cycle. Effect on model of healthy control data (gray) of slowing Na channel inactivation by 37% (black) is shown for I/V relationship (A), strength-duration time constant (B), threshold electrontonus (C) and recovery cycle (D). E shows the best discrepancy reductions between healthy control model and post-infusion data obtainable by changing single model parameters. (Aah = rate constant

Na channel inactivation, Aas = rate constant slow K channel activation, Cah = slope factor Na channel inactivation, GKsN = conductance nodal slow K channels, Bah = half-activation voltage Na channel inactivation, Aam = rate constant Na channel activation, Bq = half-activation voltage HCN channels, GKfN = conductance nodal fast K channels, GH = conductance HCN channels, Can = slope factor fast K channels, Cam = slope factor Na channel activation, PNaN = permeability nodal Na channels, Bam = half-activation voltage Na channel activation, GLk = internodal leak conductance, GBB = Barrett-Barrett conductance)

Fig. 7. The effects of slowing sodium channel inactivation on the recovery cycle. A) The recovery cycles of the 12 post-infusion recordings superimposed, B) Modeled recovery cycles for inactivation rates from 90% to 30% of normal, C,D) Modeled action potential waveforms corresponding to recovery cycles in B, with different scaling to show action potential broadening (C) and increased positive afterpotentials corresponding to subexcitability (D). Action potentials truncated in D.

Fig. 8. Correlation coefficient for correlations between total time-adjusted dose of oxaliplatin and A) superexcitability, B) The two most abnormal sensations induced by oxaliplatin. C and D show scatter plots of values for superexcitability and cold cylinder pricking, respectively, versus estimated dose/area for a half-life of 10 days. Filled symbols indicate post-infusion examination and open symbols indicate recovery examination.

Tables

Table 1. Clinical characteristics.

Characteristics	**n(%) or mean ±SD**
Females	6 (50)
Age (years)	57.2 ± 12
Height (cm)	172.3 ± 13
Weight (kg)	78.0 ± 24
Disease stage	
II	3 (25)
III	8 (67)
IV	1 (8)
Treatment cycles	
1 cycle	2 (17)
2 cycles	8 (67)
3 cycles	2 (17)
Single dose (mg)	220.3 ± 39
Patients receiving full dose (130 mg/m^2)	9 (75)
Patients receiving reduced dose (97.5 mg/m^2)	3 (25)
Patients reduced in dose	4 (33)
Due to neuropathy	0 (0)
Incomplete post-operative recovery	4 (33)
Examination, days after treatment	
1 day	5 (42)
2 days	2 (17)
3 days	5 (42)

Table 2. Symptoms after oxaliplatin treatment and recovery.

Symptom	**Post-infusion examination (n(%) or mean ± SD)**	**Recovery examination (n(%) or mean ± SD)**
Patients (n)	12	11
Patients with pain (24hrs)	4 (33)	0 (0.0)
Hands	2 (17)	-
Feet	1 (9)	-
Throat	2 (17)	-
Intensity of pain,(NRS)*	3.8 ± 2	-
Patients with abnormal sensations (24hrs)	11 (92)	2 (18)
Hands	11 (92)	1 (9)
Feet	4 (33)	0 (0)
Throat	10 (83)	1 (9)
Intensity of abnormal sensations (NRS)*	5.3 ± 3	1.5 ± 0.7
Most common symptoms in upper extremity**		
Tingling or pins and needles	12 (100)	5 (45)
Burning pain or discomfort with cold	11 (92)	5 (45)
Most common symptoms in lower extremity**		
Tingling or pins and needles	5 (42)	1 (9)
Burning pain or discomfort with cold	3 (25)	0 (0)
Heavy legs	6 (50)	2 (18)
Most common symptoms in face/mouth**		
Jaw pain	5 (42)	0 (0)
Throat discomfort	12 (100)	5 (45)
Tingling in mouth	6 (50)	1 (9)
Burning pain or discomfort in eyes	4 (33)	0 (0.0)
Difficulty with speech	4 (33)	0 (0.0)
NPSI score (0-100)***	22.3 ± 16	1.0 ± 2
Evoked pain (0-10)	2.6 ± 3	0.2 ± 0.3
Pressing (deep) spontaneous pain (0-10)	0.5 ± 0.8	0.0 ± 0
Paroxysmal pain (0-10)	3.0 ± 3	0.1 ± 0.3
Pins and needles/tingling (0-10)	3.7 ± 2	0.1 ± 0.2
Burning superficial pain (0-10)	0.8 ± 2	0.0 ± 0

*Mean intensity and sd of patients who reported pain and paresthesia.

**Oxaliplatin-specific questionnaire

***NPSI questionnaire. NPSI: Neuropathic Pain Symptom Inventory.

Table 3. Nerve excitability measurement in motor axons.

	Healthy controls (n = 16)	**Patients post-infusion** (n = 11)[a]	**Patients recovery** (n = 11)[a]	**Difference** (n = 11)[b]
Stimulus-response and strength-duration properties				
Stimulus (mA) for 50% maximal CMAP[c]	4.74 ×/÷ 1.08	**6.97 ×/÷ 1.12****	5.78 ×/÷ 1.1	**1.21 ×/÷ 1.06****
Peak CMAP (mV)[c]	8.83 ×/÷ 1.08	9.05 ×/÷ 1.11	8.74 ×/÷ 1.09	1.04 ×/÷ 1.09
Strength-duration time constant (ms)	0.46 ± 0.02	0.41 ± 0.02	0.49 ± 0.03	**-0.08 ± 0.02****
Rheobase (mA)[c]	3.1 ×/÷ 1.09	**4.77 ×/÷ 1.13****	3.72 ×/÷ 1.1*	**1.28 ×/÷ 1.06****
Threshold electrotonus				
TEd^{40}(peak) (%)	67.61± 1.3	68.5 ± 1.0	67.8 ± 0.7	0.7 ± 1.1
TEd^{40}(90-100ms) (%)	42.9 ± 0.8	45.2 ± 1.0	44.0 ± 0.7	1.2 ± 0.7
TEd^{20}(peak) (%)	37.9 ± 1.1	38.9 ± 0.9	38.2 ± 0.5	0.7 ± 0.9
TEd(undershoot)(%)	-20.1 ± 1.0	-17.9 ± 0.6	-19.3 ± 0.8	1.4 ± 0.8
TEh^{40}(20-40ms) (%)	-93.2 ± 2.5	-95.1 ± 2.9	-97.8 ± 2.7	2.6 ± 2.7
TEh^{40}(90-100ms) (%)	-118.9 ± 5.8	-129.6 ± 7.1	-124.5 ± 4.5	-5.0 ± 4.2
Current-threshold properties				
Resting I/V slope	0.591 ± 0.020	0.557 ± 0.022	0.572 ± 0.013	-0.015 ± 0.019
Minimum I/V slope	0.259 ± 0.013	0.281 ± 0.014	0.262 ± 0.015	**0.019 ± 0.006****
Hyperpolarising I/V slope	0.394 ± 0.012	**0**.441 ± 0.017*	0.411 ± 0.015	0.030 ± 0.014
Recovery Cycle				
RRP (ms) [c]	3.13 ×/÷ 1.03	3.33 ×/÷ 1.04	3.12 ×/÷ 1.02	1.55 ×/÷ 1.43
Superexcitability (%)	-23.2 ± 1.7	**-10.2 ± 1.9******	-19.8 ± 1.1	**9.6 ± 1.6*****
Subexcitability (%)	14.2 ± 0.9	**23.2 ± 2.5*****	15.1 ± 1.9	**8.0 ± 2.1****

Comparison between nerve excitability measurements in motor axons of patients and controls. Values are mean ± SEM, except for 3 measurements (indicated by [c]) which were normalized by log conversion and values are geometric mean ×/÷ standard error expressed as a factor. TEd^{40}(peak)% = Peak percentage threshold reduction in threshold electrotonus with depolarizing current, 40% of unconditioned threshold. TEh^{40}(20-40ms) = Mean threshold reduction 20-40 ms after start of 40% hyperpolarizing current. RRP = relative refractory period.

[a] Asterisks indicate probability of difference from healthy controls by two-tailed *t*-test.

[b] Asterisks indicate probability of difference between two patient recordings by two-tailed paired *t*-test.
[a,b] * = $P < 0.05$, ** = $P < 0.01$, *** = $P < 0.001$, **** = $P < 0.0001$.

Table 4. Nerve excitability measurements in sensory axons.

	Healthy controls (n = 16)	**Patients post-infusion** (n = 11)[a]	**Patients recovery** (n = 11)[a]	**Difference** (n = 11)[b]
Stimulus-response and strength-duration properties				
Stimulus (mA) for 50% maximal CSAP[c]	4.80 ×/÷ 1.06	**6.48 ×/÷ 1.10****	5.34 ×/÷ 1.07*	1.21 ×/÷ 1.06*
Peak CSAP (μV)[c]	28.1 ×/÷ 1.12	36.3 ×/÷ 1.62	21.0 ×/÷ 1.18	1.73 ×/÷ 1.70
Strength-duration time constant (ms)	0.566 ± 0.015	**0.464 ± 0.025****	0.566 ± 0.04	**-0.10 ± 0.03****
Rheobase (mA)[c]	2.07 ×/÷ 1.07	**3.19 ×/÷ 1.13****	2.37 ×/÷ 1.08*	**1.35 ×/÷ 1.08****
Threshold electrotonus				
TEd^{40}(peak) (%)	61.7 ± 0.8	62.9 ± 0.7	62.3 ± 0.8	0.6 ± 0.9
TEd^{40}(90-100ms) (%)	48.1 ± 1.1	47.6 ± 1.2	47.5 ± 1.0	0.1 ± 1.2
TEd^{20}(peak) (%)	41.7 ± 1.4	41.2 ± 0.9	42.2 ± 1.3	-1.0 ± 1.1
TEd(undershoot)(%)	-20.7 ± 0.9	-19.5 ± 0.5	-21.6 ± 0.9	2.1 ± 0.7*
TEh^{40}(20-40ms) (%)	-107.8 ± 3.3	-107.2 ± 3.4	-111.5 ± 4.6	4.3 ± 2.3
TEh^{40}(90-100ms) (%)	-140.6 ± 6.5	-144.4 ± 5.5	-149.0 ± 7.6	4.5 ± 3.6
Current-threshold properties				
Resting I/V slope	0.546 ± 0.018	0.550 ± 0.028	0.572 ± 0.013	-0.003 ± 0.013
Minimum I/V slope	0.245 ± 0.011	0.277 ± 0.012	0.262 ± 0.015	0.019 ± 0.010
Hyperpolarising I/V slope	0.457 ± 0.033	0.464 ± 0.029	0.411 ± 0.015	0.005 ± 0.029
Recovery Cycle				
RRP (ms) [c]	3.49 ×/÷ 1.05	2.95 ×/÷ 1.06*	3.12 ×/÷ 1.02	0.94 ×/÷ 1.06
Superexcitability (%)	-16.8 ± 1.5	-16.6 ± 1.5	-19.6 ± 0.7	3.0 ± 1.2*
Subexcitability (%)	10.0 ± 0.6	10.5 ± 0.8	15.1 ± 1.9	1.3 ± 0.9

Comparison between nerve excitability measurements in sensory axons of patients and controls. Values are mean ± SEM, except for 3 measurements (indicated by [c]) which were normalized by log conversion and values are geometric mean ×/÷ standard error expressed as a factor. CSAP = compound sensory action potential. Other abbreviations as in Table 3.

[a] Asterisks indicate probability of difference from healthy controls by two-tailed *t*-test.

[b] Asterisks indicate probability of difference between two patient recordings by two-tailed paired *t*-test. [a,b] * = $P < 0.05$, ** = $P < 0.01$.

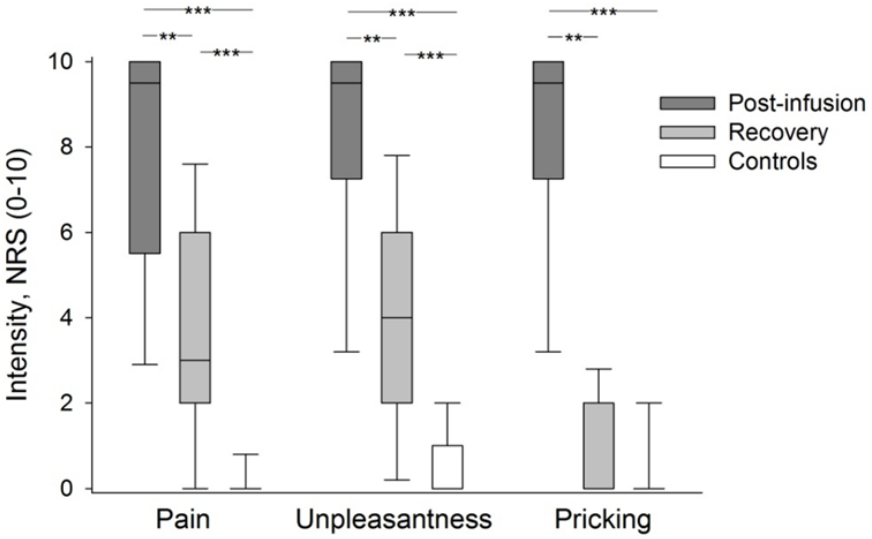

Figure 1

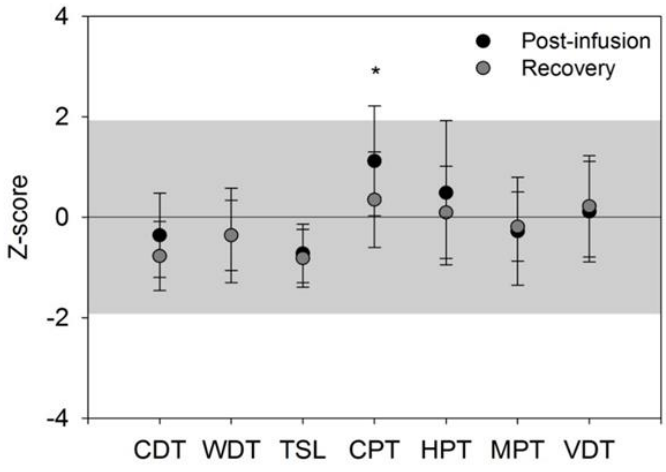

Figure 2

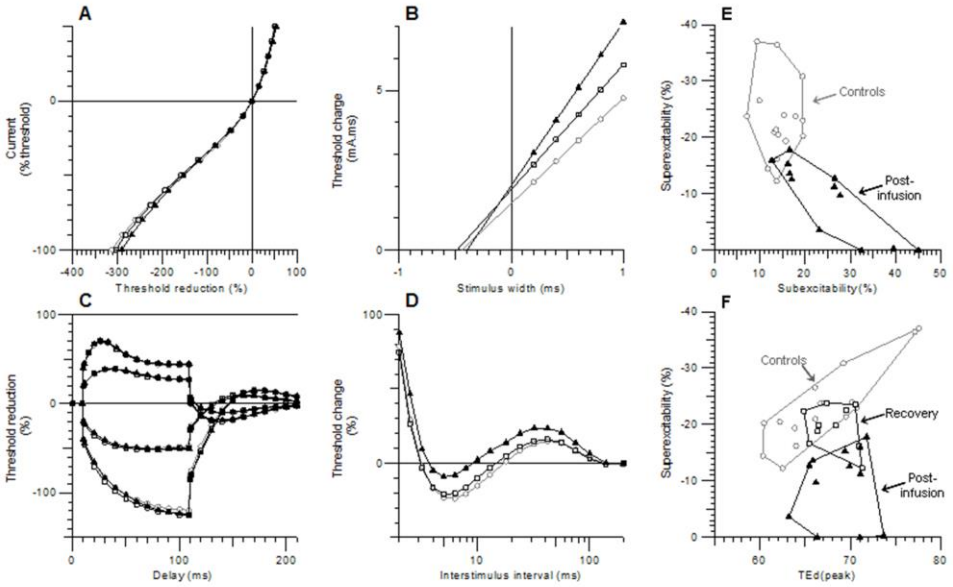

Figure 3

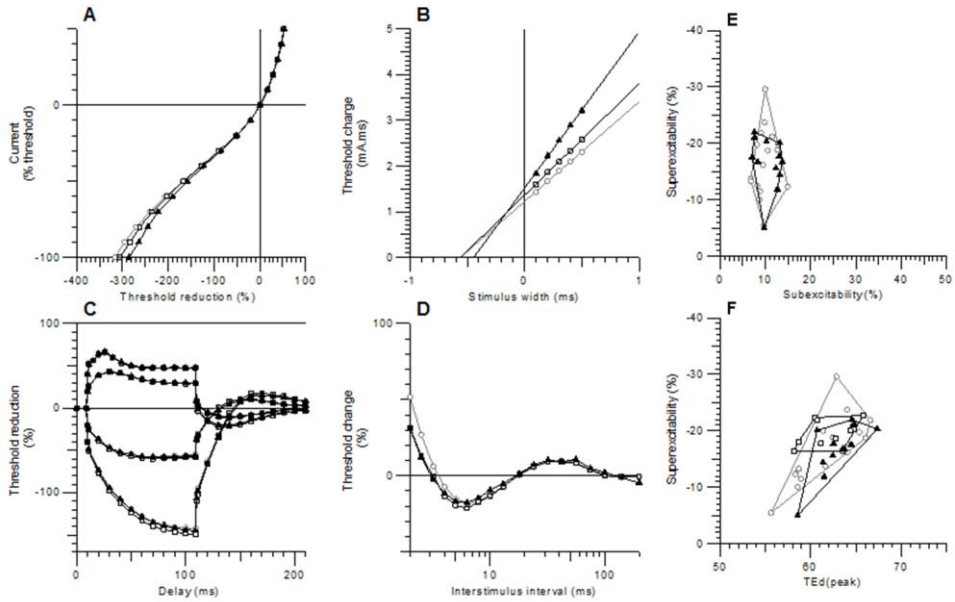

Figure 4

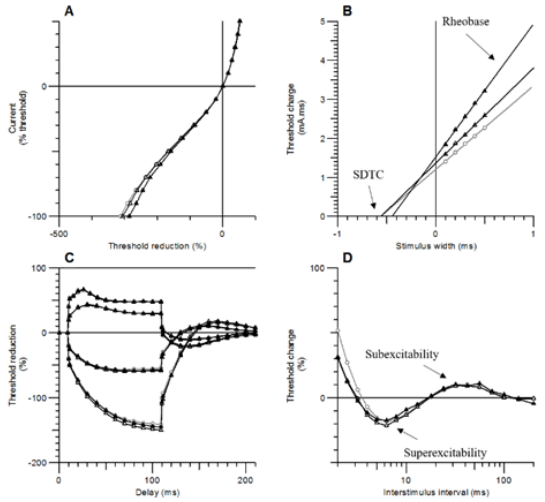

Figure 5

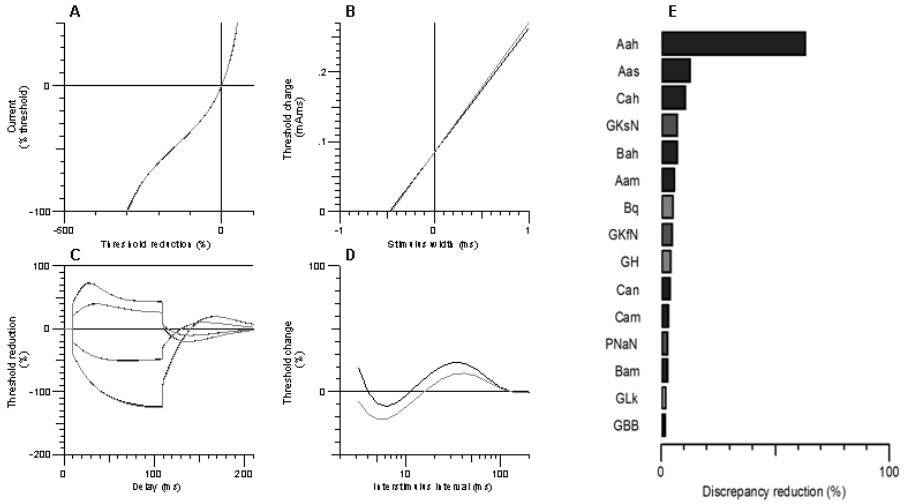

Figure 6

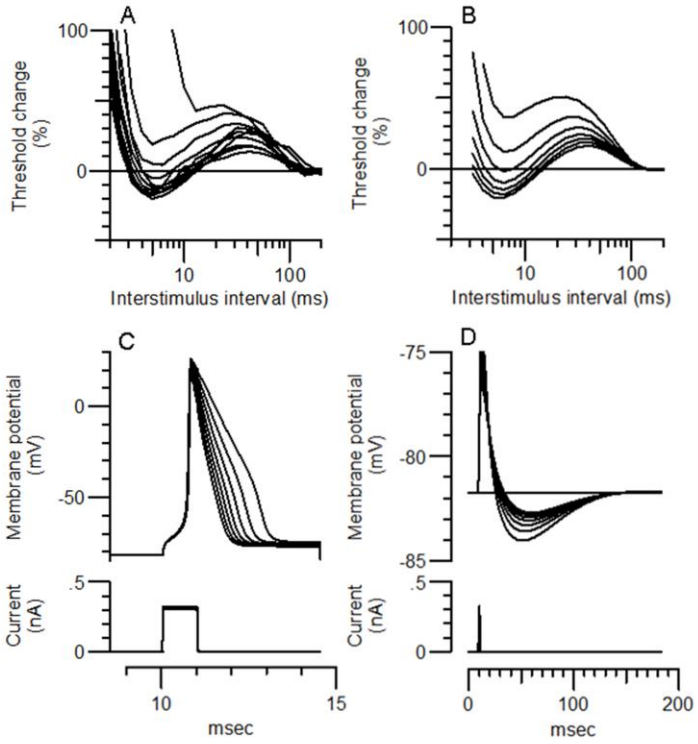

Figure 7

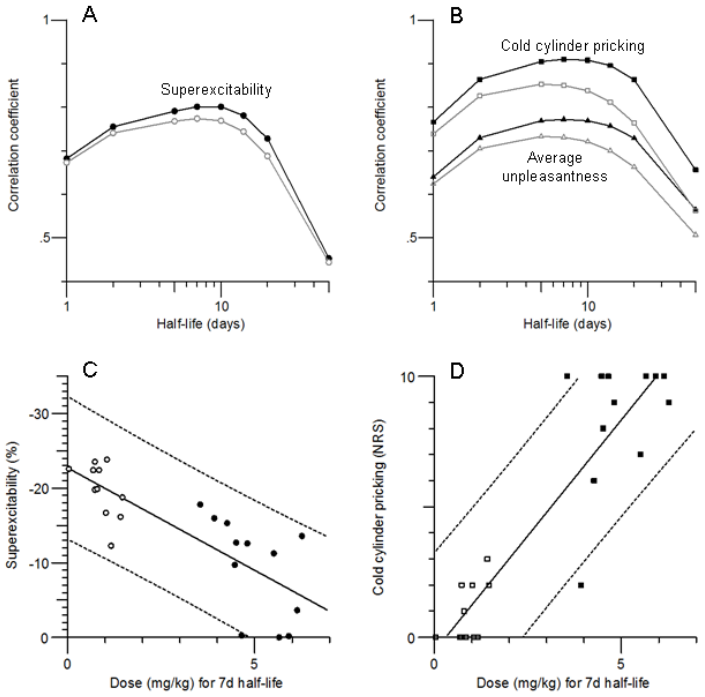

Figure 8